Functional & Integrative Genomics (2023) 23:314
https://doi.org/10.1007/s10142-023-01237-3

ORIGINAL ARTICLE

PFT-α protects the blood-brain barrier through the Wnt/β-catenin pathway after acute ischemic stroke

Haitao Zhang[1] · Deyong Du[1] · Xiaoning Gao[1] · Xiaoling Tian[1] · Yongqiang Xu[1] · Bo Wang[1] · Shoujuan Yang[2] · Pengfei Liu[1] · Zefu Li[1]

Received: 25 May 2023 / Revised: 15 September 2023 / Accepted: 18 September 2023 / Published online: 30 September 2023
© The Author(s), under exclusive licence to Springer-Verlag GmbH Germany, part of Springer Nature 2023

Abstract

The dysfunction of blood-brain barrier (BBB) plays a pivotal role in brain injury and subsequent neurological deficits of ischemic stroke. The current study aimed to examine the potential correlation between p53 inhibition and the neuroprotective effect of on the BBB. Rat middle cerebral artery occlusion and reperfusion model (MCAO/R) and oxygen-glucose deprivation/re-oxygenation model (OGD/R) were employed to simulate cerebral ischemia-reperfusion (CI/R) injury occurrence in vivo and in vitro. mNSS and TTC staining were applied to evaluate neurological deficits and brain infarct volumes. Evans blue (EB) staining was carried out to examine the permeability of BBB. RT-qPCR and Western blot to examine the mRNA and protein levels. Cell viabilities were detected by CCK-8. Flow cytometry and ELISA assay were employed to examine apoptosis and neuroinflammation levels. TEER value and sodium fluorescein were carried out to explore the permeability of HBMEC cells. PFT-α inhibited P53 and promoted the expression of β-catenin and cyclin D1, which were reversed by DKK1. PFT-α inhibited neurological deficits, brain infarct volume, neuroinflammation, apoptosis, and BBB integrity than the MCAO/R rats; however, this inhibition was reversed by DKK1. PFT-α promoted OGD/R-induced cell viability in NSCs, and suppressed inflammation and apoptosis, but DKK1 weakened the effect of PFT-α. PFT-α increased OGD/R-induced TEER values in cerebrovascular endothelial cells, inhibited sodium fluorescein permeability, and increased the mRNA levels of tight junction protein, but they were all attenuated by DKK1. PFT-α protects the BBB after acute ischemic stroke via the Wnt/β-catenin pathway, which in turn improves neurological function.

Keywords CI/R injury · p53 · WNT signaling pathway · BBB · Neuroinflammation

Introduction

Stroke is the primary source of morbidity, mortality, and long-term disability around the world, with approximately 40 million patients reported to suffer long-term disability due to stroke each year (Shi et al. 2021, Qiao et al. 2023). Cerebral ischemia (CI) is a disease characterized by intracranial ischemia and hypoxia, accounts for more than 85% of stroke patients (Li et al. 2022b), and is associated with about 15 million new cases and 30% mortality each year (Huang et al. 2021). Although mechanical embolization or intravenous thrombolytic agents combined with alteplase are currently effective strategies for the clinical management of CI (Xie et al. 2022), reperfusion of CI (CI/R) tends to restore blood flow while exacerbating brain tissue damage, disrupting the blood-brain barrier (BBB), and weakening neurological function, which in turn triggers poor prognosis for CI patients (Liu et al. 2020a).

Haitao Zhang and Deyong Du contributed equally to this work.

✉ Shoujuan Yang
yangshoujuan01@126.com

✉ Pengfei Liu
byfylpf01@163.com

✉ Zefu Li
bylzf6688@163.com

[1] Department of Neurosurgery, Binzhou Medical University Hospital, No. 661, Huanghe 2nd Road, Binzhou 256603, China

[2] Department of Cardiology, Binzhou Medical University Hospital, No. 661, Huanghe 2nd Road, Binzhou 256603, China

Consequently, effective therapeutic strategies to combat cerebral ischemia-reperfusion (CI/R) injury are urgently needed, and it is particularly vital to promote the health recovery of CI patients.

BBB injury has been identified as one of the key pathological mechanisms of ischemic stroke (Cao et al. 2016). And BBB is a highly specialized endothelial tissue whose function is governed by the brain microvascular endothelial to precisely control cerebral homeostasis and maintains neurological function. Moreover, when CI/R injury, brain endothelial cell permeability is elevated, BBB integrity is impaired, and a large number of harmful substances and fluids enter the brain parenchyma, leading to the development of brain edema and neurological deficits. Therefore, it has significant opinion to explore the BBB damage for the treatment of CI/R damage. The critical function of the WNT signaling pathway in CNS ontogenesis, progression, and differentiation has been widely recognized (Liu et al. 2013). Previous studies have confirmed that WNT3a, β-catenin, and cyclin D1 protein levels of the WNT signaling pathway are suppressed significantly in CI/R injury (Wisniewska 2013). A conditioned medium for AMSC exerts CI/R injury neuroprotective effects by activating the WNT pathway (Nazarinia et al. 2021). During CI/R injury, the blood-brain barrier integrity was weakened in mice deficient with Gpr124, which was a specific activator of the WNT signaling pathway, and this was reversed when activation of the β-catenin (Chang et al. 2017). Furthermore, Dickkopf-1 (DKK1), a negative regulator in the WNT pathway, significantly inhibited WNT by suppressing the expression of β-catenin and GSK-3β proteins. Previous studies confirm that DDK1 inhibits neuronal apoptosis in the hippocampal tissue of CI/R injury rats (Liu et al. 2013); however, the exact regulatory mechanism was unknown. More importantly, our previous study has demonstrated the protection of the p53 inhibitor against CI/R injury (Liu et al. 2021). P53 is a widely characterized tumor suppressor, and its activation affects metabolism, DNA repair, and apoptosis. A primary target of p53 is the WNT signaling pathway (Yang et al. 2019). Our previous research also revealed a significant upregulation of key proteins in the WNT signaling pathway in rats with CI/R injury, where p53 was suppressed (Liu et al. 2021), but whether p53 reduction exerts protection against CI/R injury through inactivation of the WNT signaling pathway is unclear.

Based on the foregoing, the present research focused on the potential function of the WNT signaling pathway in suppressing p53 and exerting anti-CI/R injury. The way in which the WNT signaling pathway is concerned with CI/R injury is examined by constructing in vivo animal models and in vitro cellular models, which may provide new perspectives for the clinical treatment of patients and targeted therapies.

Materials and methods

Ethics statement

Animal care was conducted in compliance with the Guidelines for Care and Use of Laboratory Animals issued by the Ministry of Science and Technology of China, and the experimental protocols were passed by the Binzhou Medical University Hospital Animals Care and Use Committee. Every effort was made to reduce the number of animals as well as their suffering.

Reagents

Recombinant human DKK1 protein (rhDKK1) obtained from R&D systems (cat# 5493-DK-010). Chloral hydrate (10%, cat# 47335-U), 2% EB solution (cat# E-22129-10G), dimethylformamide solution (cat# D4551), 2% 2,5-triphenyl tetrazolium chloride solution (TTC, cat ## T8877), and 4% paraformaldehyde (cat# P6148) were obtained from Sigma-Aldrich. TRIzol (cat# 15596018) reagent was obtained from Invitrogen. HiFiScript cDNA Synthesis kit (cat# CW2569M) and UltraSYBR Mixture Kit (cat# CW2602M) were obtained from CW Biotech. Protein lysate RIPA solution (cat# P0013B) and BCA protein concentration assay kit (cat# P0009) were obtained from Beyotime. Polyvinylidene fluoride (PVDF) membrane obtained from Merck Millipore (cat# K5MA6539B). The antibodies against p53 (cat# 9282), cyclin D1 (cat# 2922), β-catenin (cat# 8480), Bcl_2 (cat# 15071), bax (cat# 2772S), and β-actin (cat# 4967S) were from cell signaling technology and were used at 1:1000 dilution. Horseradish peroxidase-coupled secondary antibody goat anti-mouse IgG (cat# SA00001-1) and goat anti-rabbit IgG (cat#SA00001-2) were obtained from Proteintech. Enhanced chemiluminescence detection kit (cat# PI32106) was obtained from Thermo-Fisher. Cell Counting Kit-8 (CCK-8, cat #CK04) was from Dojindo. 0.25% trypsin (cat# 25200-056) was from Thermo Fisher Scientific. Penicillin/streptomycin (1%; cat# 15140-122) DMEM/F12 medium (cat# C11320033), B27 supplement (cat# 17504044), and neurobasal medium (cat #12348017) were from Gibco. EGF (cat# AF-100-15) and β-FGF (cat#100-18b) were from Peprotech. Annexin V-FITC: FITC Apoptosis Detection kit (cat: 556570) was obtained from BD Pharmingen. Interleukin 6 (IL-6) ELISA kit (cat#E-EL-R0015c) and tumor necrosis factor α (TNF-α) ELISA kit (cat# E-EL-R2856c) were obtained from Elabscience. Human brain microvascular endothelial cells (HBMECs) were purchased from ScienCell Research Laboratories (cat# 1000).

Animals

Sixty-eight adult male Sprague-Dawley (SD) rats were obtained from the Shanghai Laboratory Animal Center of the Chinese Academy of Sciences, which was maintained at 250 ± 30 g. They were housed in a laboratory animal center with 22–25°C, 12-h light/dark cycle, 60% humidity, and free access to food and water. Experiments were performed after 1 week of adaptation to this environment, and the rats were normal before the experiments and were free of pain, infection, and neurological deficits.

Model construction of middle cerebral artery occlusion and reperfusion (MCAO/R)

To trigger CI/R injury in rats, a middle cerebral artery occlusion and reperfusion (MCAO/R) model was established by a modified nylon suture method according to a previous study (Guo et al. 2021). Briefly, rats acclimated to the feeding environment were deeply anesthetized with 30 mg/kg chloral hydrate (10%) after 12 of fasting. The skin of the neck was incised along the midline of the rat, the skin and muscle were carefully peeled off, and the right common carotid artery (CCA), external carotid artery (ECA), and internal carotid artery (ICA) were exposed under the microscope. ICA was subsequently inserted through the right ECA with 6-0 nylon wire to a depth of 16–20 mm to occlude the middle cerebral artery (MCA) in rats. Transcranial laser Doppler determined that the MCAO model was considered successfully constructed when cerebral blood flow was reduced by 80%. After 2 h of ischemia, sutures were removed, and blood flow was restored. During the experiment, the rats were placed on a heating blanket at about 37 °C and maintained at a body temperature of 37 ± 0.5 °C. The anesthetized awakened rats were returned to their cages and resumed free feeding and drinking. After successful modeling, 4 rats died, ensuring that at least 16 individuals in the group survived (no rats died in the sham group).

Grouping and medication management

Sixty-forty SD rats ($n = 16$ per group) were created as follows: (1) sham group (received the same surgery without occlusion of the middle carotid artery); (2) MCAO/R group (received MCAO/R and same volume of 0.9% PBS 10 ml/kg); (3) MCAO/R+PFT-α group (PFT-α is a p53 inhibitor, and 3μl PFT-α [10μM] was injected intracerebrally at 24 h after MCAO/R and continued for 3 days); (4) MCAO/R + PFT-α + DKK1 (DKK1 acted as an inhibitor of WNT signaling pathway was injected 5 μL of 1 μg/μL DKK1 into the ventricles by stereotaxic instrumentation, as in the PFT-α protocol). The time and number of rats of MCAO/R + PFT-α + DKK1 was shown in Supplementary Figure 1. Recombinant human DKK1 protein was dissolved in sterile PBS and configured at 1 μg/μL as previous research (Zhang et al. 2008). Rats were fixed on a stereotactic apparatus (stereotactic coordinates were dorsoventral: dorsal-ventral (−3.5 mm) from bregma, medio-lateral (1.5 mm), and anterior-posterior (−0.92 mm) to complete intracerebroventricular injection by a microinjector. To prevent leakage, the needle was slowly withdrawn after 5 min of injection.

Neurological deficit evaluation

The modified Neurological Severity Score (mNSS) was adopted to evaluate the degree of neurological deficits in rats. After 24 h of MCAO/R, mNSS was assessed by two unknowingly grouped experimenters at 1, 3, 5, and 7 days after surgery. Motor, touch, abnormal behavior, sensory, reflex, and balance items were included, with scores ranging from 0 to 18, with higher scores resulting in more severe neurological deficits (Pu et al. 2022). And failure to test or test reflexes was scored one point (Li et al. 2022a).

After assessment of neurological deficits on day 7, except for the four rats tested for blood-brain barrier integrity assay, rats were sacrificed by intraperitoneal injection of 10% chloral hydrate at an anesthetic dose of 300 mg/kg and cervical dislocation according to the previous method (Liu et al. 2020b, Lin et al. 2020). Subsequent experiments were performed.

BBB integrity assay

Randomly selected 4 rats per group at 7 days after MACO/R. Evans blue (EB) staining was carried out to examine the permeability of BBB. 2% EB solution was injected into the rats at 4 mL/kg through the tail vein for 4 h, followed by 10% chloral hydrate anesthesia and left ventricular perfusion with pre-chilled PBS solution to remove EB solution. The cervical vertebrae were dislocated and executed, and the bilateral cerebral hemispheres were weighed and incubated in 1 mL/100 mg dimethylformamide solution at 60 °C for 24 h. The solution was then centrifuged for 10 min at 1000 g. The EB solution was detected spectrophotometrically at 620 nm.

Cerebral infarction volume

Randomly selected 4 rats per group at 7 days after MACO/R. Rat brain tissue was collected on ice and refrigerated at −20 °C for 30 min, and then quickly removed and cut into 5 consecutive coronal sections of 2 mm thickness. Then, the sections were completely immersed in 2% TTC solution and incubated at room temperature for 20 min in the dark. Paraformaldehyde (4%) was fixed overnight, and the area of unstained brain infarcts was measured by the Image J software, and the infarct volume was calculated by the following

equation: Infarct volume (%) = [(normal hemisphere volume − the non-infarct volume of infarct side)/normal hemisphere volume] × 100%.

Brain water content measurement

Randomly selected 4 rats per group at 7 days after MACO/R. The brains of rats were collected, and the bilateral cerebral hemispheres were separated and weighted. The brains were then dried at 100 °C for 48 h, followed by weighing of the bilateral hemispheres. Brain water content (%) = (wet weight-dry weight)/ wet weight × 100%.

Reverse transcriptase quantitative polymerase chain reaction (RT-qPCR)

Randomly selected 4 rats per group at 7 days after MACO/R. The penumbra area of the ischemic hemisphere was dissected for cortical tissue, and the corresponding cortical area was isolated from the non-ischemic contralateral hemisphere. TRIzol was used to isolate RNA from tissues. RNA (500 ng) was reversed to cDNA using HiFiScript cDNA Synthesis kit when the A260/280 of the extracted RNA was confirmed by a spectrophotometer at 1.8–2.2. Then, cDNA, primers, and reagents from the UltraSYBR Mixture Kit were mixed into a 20 μL system and RT-qPCR amplification was carried out in triplicate on an ABI 7300 real-time PCR system. β-actin was used as an internal reference in RT-qPCR, and the $2^{-\Delta\Delta Ct}$ method was adapted to calculate the mRNA expression.

Western blotting

Randomly selected 4 rats per group at 7 days after MACO/R. Protein phosphatase inhibitors were added to the protein lysate RIPA. Cortical tissue was snap-frozen in liquid nitrogen and then broken up in a mortar, followed by the addition of RIPA reagent for 60 min at 4 °C. The supernatant lysate was collected by centrifugation, and the BCA protein concentration assay kit assessed the concentration. Protein (25 μg) was taken for electrophoresis at 80 V for 120 min, followed by transferring the protein to PVDF membranes at 90 V for 100 min, and closed with 5% skim mile buffer for 2 h, then incubated with primary antibody overnight at 4 °C. The primary antibodies such as p53, cyclin D1, β-catenin, bcl_2, bax, and β-actin were diluted. Membranes were washed three times with TBST solution for 10 min and co-incubated with horseradish peroxidase-coupled secondary antibodies for 2 h at room temperature. After washing the membrane three times with TBST, the protein bands were visualized with an enhanced chemiluminescence detection kit, and their optical density was quantified with the Image J software.

Isolation and culture of neural stem cells (NSCs)

As in our previous study, neural stem cells (NSCs) were isolated from the cortical and ganglionic bulge sites of SD fetal rats (18 days old). Brain tissue was dissected and mechanically separated in PBS solution supplemented with 2% penicillin/streptomycin and digested with 0.25% trypsin for 30 min. The dissociated single-cell suspension was inoculated in 6-well plates coated with poly-L-lysine and maintained in DMEM/F12 medium containing 25 mM L-glutamine, 20 ng/ml β-FGF, 20 mg/ml EGF, 2% B27, and 1% penicillin/streptomycin in an incubator at 37 °C, 95% O_2, and appropriate humidity. Passaging was performed after about 7 days, and MAP2 antibody was confirmed that neuronal purity exceeded 98%, followed by in vitro experiment.

Oxygen-glucose deprivation/re-oxygenation (OGD/R)

Oxygen and glucose deprivation/re-oxygenation (OGD/R) of NSCs was employed as an in vitro model of neural damage with CI/R injury. The medium of NSCs was changed to NBM-B27 which did not contain glucose and the cells were transferred to anaerobic conditions (37 °C, 95% N_2, and 5%CO_2); after 8 h, the medium was changed to DMEM/F12 medium and returned to the normoxic environment to end OGD. PFT-α (10 μL) or/and DKK1 (100 μg/ml) was supplemented during the OGD.

Cell viability and apoptosis analysis

CCK-8 regent was applied to explore cell viability. NSCs were inoculated in 96-well plates after different treatments, and the medium was mixed with CCK-8 in a 10:1 ratio and subsequently added to the cells. The absorbance at 450 nm was detected by an enzyme marker after an additional 1 h incubation in a 37 °C-incubator containing 5% CO_2.

Apoptosis flow cytometry assay was performed. EDTA-free trypsin collected cells were centrifuged, washed with pre-cooled PBS, and resuspended with 100 μL of membrane-linked protein binding buffer. Incubated 5 μL Annexin V-FITC and 5 μL propidium iodide (PI) staining for 15 min in darkness, followed by replenishment of membrane association protein buffer to 500 μL, and detection the number of apoptotic cells on a flow cytometer.

Enzyme-linked immunosorbent assay (ELISA)

Lysed rat cortical tissue or cell supernatant was collected, and secreted levels of neuroinflammatory factors such as IL-6 and TNF-α were measured with the help of commercial ELISA kits. Briefly, the bottom of the kit is coated with specific IL-6 and TNF-α. The supernatant is added to the

bottom of the kit and incubated in an incubator for 4 h to wash the unbound antibody, followed by the catalytic substrate, and the OD 450 nm was detected by adding the termination solution after incubation at room temperature.

Endothelial cell permeability assay

HBMECs were cultured in a DMEM complete medium containing 1% penicillin/streptomycin. OGD induction was performed. Transendothelial electrical resistance (TEER) assay by cellular resistivity meter to assess barrier integrity. According to previous studies (Nakada-Honda et al. 2021), the fibronectin-coated insert with a pore size of 0.4 mm was grown to confluence and inserted into the cell resistivity meter. To ensure the accuracy of the assay, the whole process was carried out at a constant temperature of 25 °C, and the measurements were repeated three times by taking three different positions.

The HBMECs were assayed for endothelial barrier permeability using sodium fluorescein as described previously (Cao et al. 2016). Briefly, Krebs-Ringer buffer (5 nM Hepes, 5.2 nM KCl, 2.2 mM $CaCl_2$, 0.2 mM $MgCl_2$, 6 mM $NaHCO_3$, and 2.8 mM glucose) containing sodium fluorescein (100 µg/mL) was added to the Transwell. Then, Transwell chambers were placed in 24-well plates. Absorbance values were subsequently measured by fluorescence spectrophotometer at OD 480 nm and 30 nm. The time of NSCs (A) and HBMECs (B) of OGD/R + PFT-α + DKK1 was shown in Supplementary Figure 2.

Statistical analysis

Experimental values were derived from at least three replicates and presented as mean ± standard deviation (SD). One-way analysis of variance (ANOVA) was performed for comparison between multiple groups, followed by Tukey's, and GraphPad Prism 9.0 was used for graphical plotting based on the data. $P < 0.05$ was regarded as a statistically significant difference.

Results

DKK1 restores the mRNA and protein levels of p53 in MCAO/R rats

We previously showed that p53 inhibitor PFT-α attenuates CI/R injury (Zhang et al. 2016). Based on PFT-α treatment of MCAO/R rats, this study was conducted with the intracerebroventricular injection of the recombinant protein DKK1, an inhibitor of the WNT signaling pathway. As illustrated in Fig. 1A–E, suppression of β-catenin and cyclin D1 as well as the elevation of p53 in MCAO/R was alleviated by PFT-αtreatment ($P < 0.05$); however, this alleviation was attenuated by DKK1 ($P < 0.05$). The findings suggest that the potential role of p53 in CI/R injury might be associated with the WNT signaling pathway.

DKK1 eliminated the alleviation of the neurological deficit by PFT-α in MCAO/R rats

Using mNSS to assess the regulation of DKK1 on neural function in PFT-α treated MCAO/R rats. After days 1, 3, 5, and 7 of model establishment, neurological deficits were significantly enhanced in MCAO/R rats and PFT-α significantly repaired neurological function, but this repair effect was reversed by DKK1 ($P < 0.05$; Fig. 2A). Additionally, MCAO/R rats had a 20% increase in brain infarct volume, which was significantly reduced by PFT-α treatment ($P < 0.05$); however, DKK1 attenuated the effect of PFT-α and increased the volume of brain infarct ($P < 0.05$; Fig. 2B). What is more, PFT-α decreased the protein and mRNA levels of the pro-apoptotic protein Bax and increased anti-apoptotic Bcl_2 in the cortical tissues ($P < 0.05$; Fig. 2C–E). However, DKK1 canceled out the protection of PFT-α on neuronal apoptosis, with increased Bax and decreased Bcl_2 ($P < 0.05$; Fig. 2C–E). Finally, the ELISA assay revealed that PFT-α reduced the elevated levels of IL-6 and TNF-α induced by MCAO/R; however, DKK1 eliminated the reduction of PFT-α on IL-6 and TNF-α ($P < 0.05$; Fig. 2F). Overall, DKK1 significantly abolished the neuroprotection of PFT-α in MCAO/R rats.

DKK1 abrogates the protective effects of PFT-α on BBB integrity in MACO/R rats

Given the potential importance of BBB damage in CI/R injury, the effect of DKK1 on BBB integrity in PFT-α-treated MCAO/R rats was subsequently analyzed. As illustrated in Fig. 3A–B, compared with the sham group, brain water content and permeability of EB were increased in rats with MCAO/R ($P < 0.05$), but PFT-α significantly inhibited this permeability, reduced brain water content, and repaired BBB damage. While this repair effect was typically reversed by DKK1 ($P < 0.05$). Additionally, the mRNA levels of both endothelial ligand proteins Zo-1, Occludin, and Claudun-5 in MCAO/R rats typically decreased compared with those in the sham group ($P < 0.05$; Fig. 3C–E), whereas PFT-α significantly promoted their expression, but DKK1 significantly suppressed the effect of PFT-α ($P < 0.05$; Fig. 3C–E).

DKK1 reversed the regulation of p53 and WNT signaling pathway key protein levels of PFT-α in OGD/R

We attempted to provide additional evidence to validate our findings. OGD/R to induce NSCs injury served to

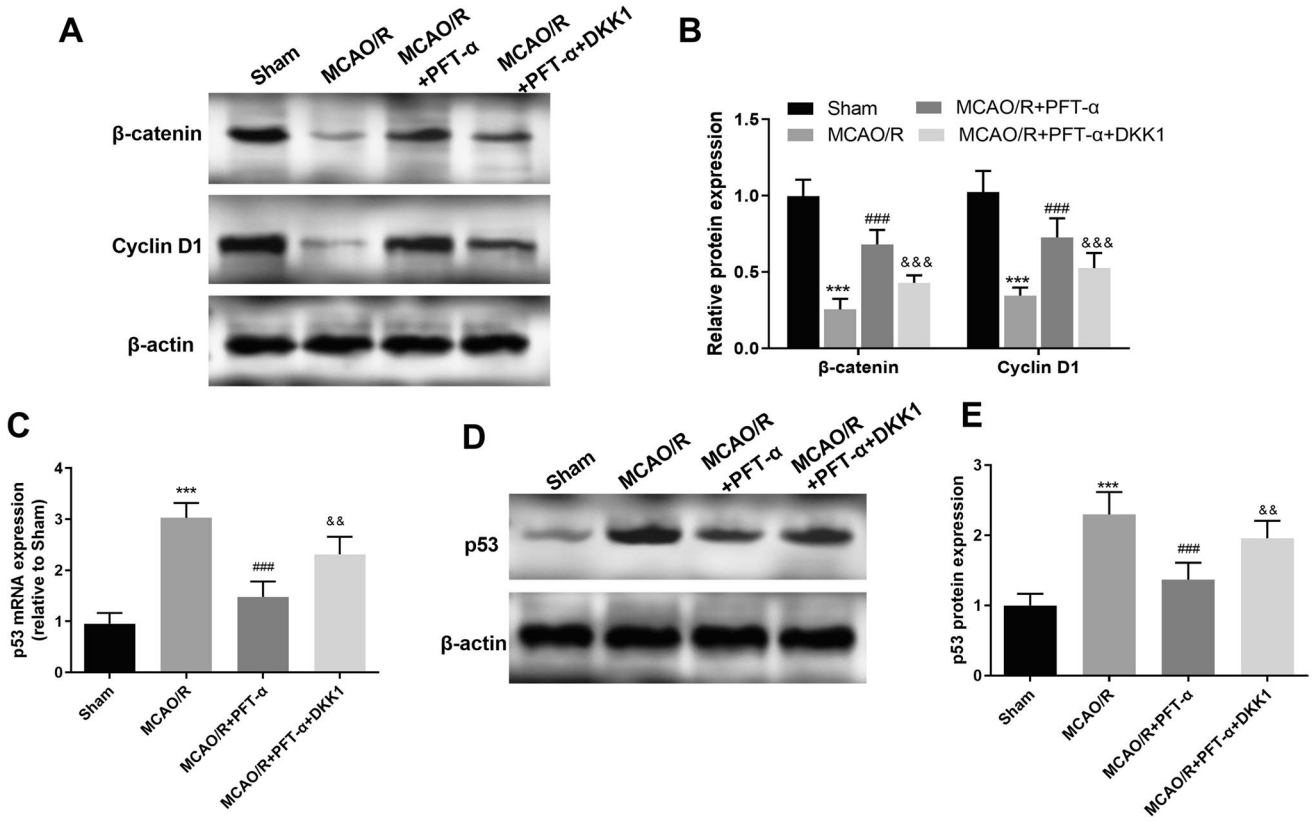

Fig. 1 DKK1 attenuated the suppression of p53 by PFT-α and the facilitation of the WNT signaling pathway. **A** Western blot detection of WNT signaling pathway key protein levels of β-catenin and cyclin D1 in MCAO/R rats after 7 days of MCAO/R. **B** Densitometric profiling of protein bands was quantified and presented as a ratio to sham after normalization by GAPDH. **C** RT-qPCR was carried out to analyze the mRNA expression of p53 after intracerebroventricular injection of DKK1 at the day 7 of MCAO/R. Western-blot analysis (**D**) and quantification (**E**) of the effect of DKK1 on p53 protein expression levels at the day 7 of MCAO/R. $n = 4$; ***$P < 0.001$ vs. Sham; ###$P < 0.001$ vs. MCAO/R; &&$P < 0.01$, &&&$P < 0.001$ vs. MCAO/R + PFT-α

mimics neural CI/R injury in vitro. NSCs with OGD/R were exposed to increasing concentrations (0–100 μg/ml) of DKK1 medium, and the cell viability gradually decreased ($P < 0.05$; Fig. 4A). Therefore, this study used 100 μg/ml DKK1 for follow-up experiments. Additionally, PFT-α promoted p53 and inhibited β-catenin and cyclin D1, but they were both partially impaired by DKK1 ($P < 0.05$; Fig. 4B–C). Our finding suggests that DKK1 also significantly reversed the regulation of p53 and WNT signaling pathway key proteins in OGD/R by PFT-α in vitro.

DKK1 diminished the protective effect of PFT-α on the cellular function of NSCs with OGD/R

CCK-8 assays confirmed a significant decrease in cell viability of NSCs in OGD/R induced, which was remarkedly restored by PFT-α treatment, but this was significantly attenuated by DKK1 ($P < 0.05$; Fig. 5A). Flow cytometry assays revealed that PFT-α also significantly inhibited the increase in OGD/R-induced apoptosis, but this inhibition was also reversed by DDK1 ($P < 0.05$; Fig. 5B). The same was true for inflammation, where OGD/R-induced inflammation was attenuation by the PFT-α, but this attenuation was reversed by DKK1, which increased the levels of inflammatory factors IL-6 and TNF-α ($P < 0.05$; Fig. 5C).

DKK1 weakened the protection of PFT-α against the permeability of OGD/R-induced HBMECs

To further investigate the potential role of DKK1 and PFT-α on BBB in CI/R injury in cells, we analyzed the changes in cell viability and permeability of HBMECs. As illustrated in Fig. 6A, OGD/R significantly reduced the cell viability of HBMECs compared to the control, but PFT-α persistently restored cell viability, but this restoration was typically reversed by DKK1 ($P < 0.05$). Additionally, OGD/R noticeably reduced the TEER value of HBMECs and increased the permeability of sodium fluorescein ($P < 0.05$), but PFT-α noticeably inhibited the effect of OGD/R, while DKK1 suppressed the effect of PFT-α ($P < 0.05$; Fig. 6B–C). Finally, mRNAs for the tight junction proteins claudin-5, occluding,

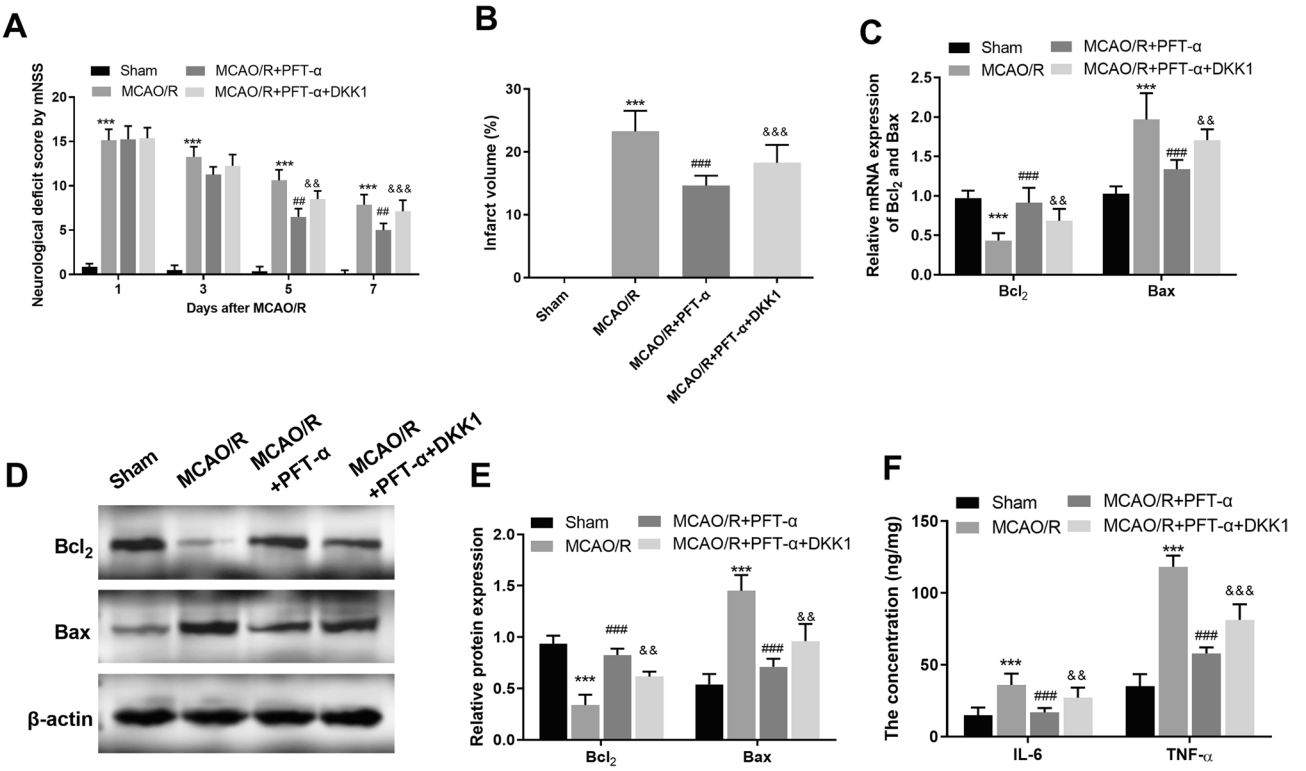

Fig. 2 DKK1 significantly abolished the neuroprotection of PFT-α in MCAO/R rats. **A** mNSS assessment of the degree of neurological deficits in rats after intracerebroventricular injection of DKK1 at the days of 1, 3, 5, 7 after MCAO/R. **B** Regulation of brain infarct volume in rats by DKK1 injection was assessed on day 7 of MCAO/R. **C**–**E** RT-qPCR and Western-blot assays were conducted to determine the mRNA and protein levels of Bax and Bcl_2 on day 7 of MCAO/R. **F** ELISA assay was conducted to examine the concentration of inflammatory factors in rats. $n = 4$; ***$P < 0.001$ vs. Sham; ###$P < 0.001$ vs. MCAO/R; &&$P < 0.01$, &&&$P < 0.001$ vs. MCAO/R + PFT-α

Zo-1 were reduced in OGD/R compared to controls, whereas PFT-α increased their levels, but this increase was persistently suppressed by DKK1 in HBMECs cells ($P < 0.05$; Fig. 6D–F).

Discussion

CI is usually caused by an interruption of the blood supply, resulting in a reduced provision of glucose and oxygen to the brain tissue. Restoration of supply can likewise cause secondary brain tissue damage (Chen et al. 2021b). Therefore, timely risk assessment, prevention, and rational treatment planning, as well as accurate neuroprotection, are essential for CI/R injury improvement. Our previous study identified the potential role of PFT-α, an inhibitor of P53, in reporting CI/R injury (Zhang et al. 2016). In the current research, we investigated the underlying mechanism based on our previous studies and found that DKK1, an inhibitor of the WNT signaling pathway, remarkedly restored p53 levels in both in vivo MCAO/R rats and in vitro OGD/R NSCs and reversed the neuroprotective effects of PFT-α on CI/R injury.

The development of CI activates multiple transcription factors and signaling pathways in the body and causes irreversible neurological damage, which in turn induces various pathophysiological changes (Wan et al. 2021). P53, a crucial tumor suppressor, exerts significant regulatory effects on both tumorigenesis and cardiovascular diseases. Additionally, p53 has been identified as a key regulator of CI/R injury (Wen et al. 2019). The involvement of p53 in the facilitation of oxidative stress and apoptosis during CI/R injury is mediated by USP29 (Hou et al. 2021). P53 also be stimulated by MEG3 to mediate ischemic neuronal death (Chen et al. 2021a). Ginkgolide attenuates CI/R injury-induced autophagy and cell death by regulating p53 (Pan et al. 2019). More importantly, our previous study has demonstrated that P53 is elevated in the in vitro MCAO/R model. Furthermore, treatment with its inhibitor PFT-α effectively reduces neurological dysfunction and brain infarct volumes in MCAO/R rats.

WNT signaling continues to be a focus of drug development and disease treatment (Jiang et al. 2022, Beni et al. 2022, Pandian et al. 2022). Meanwhile, the WNT signaling pathway is a primary target of p53, and the loss

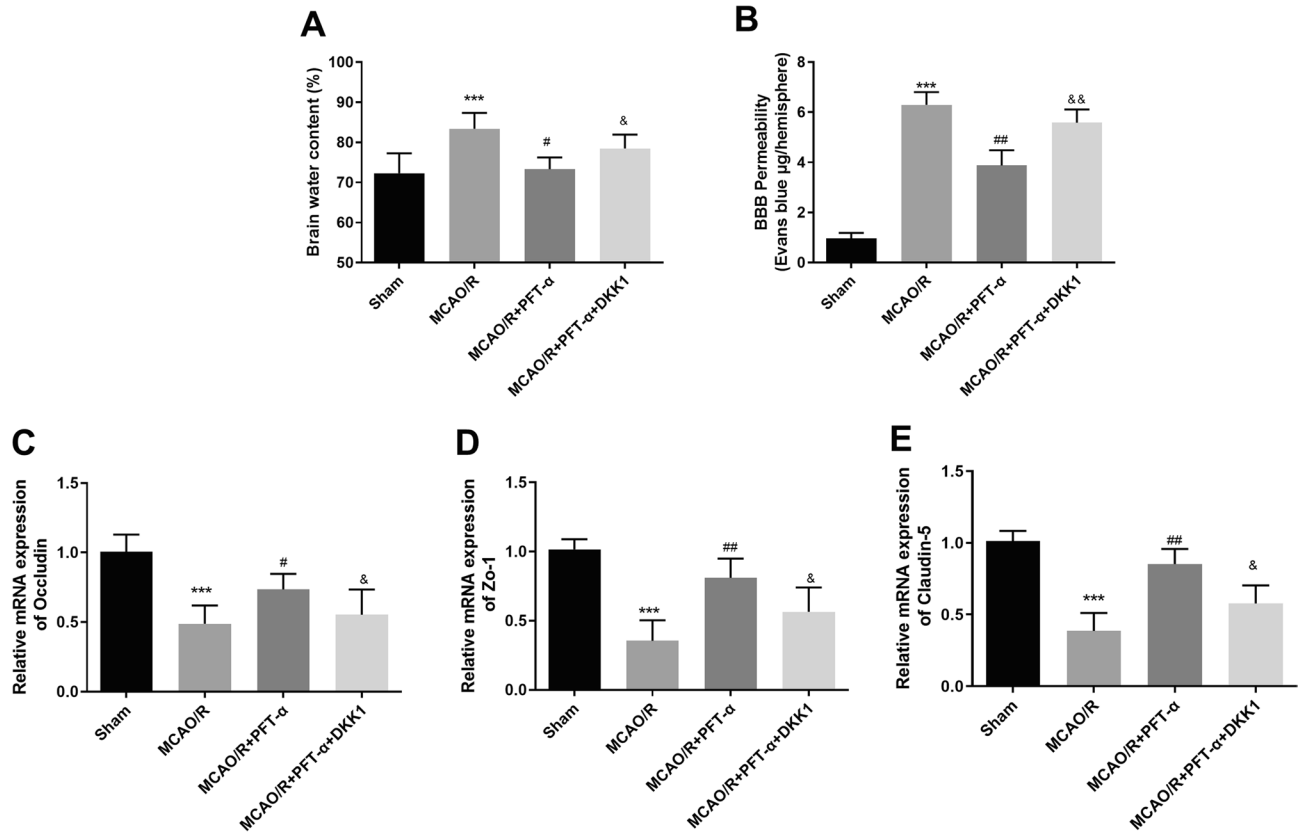

Fig. 3 DKK1 abrogates the protective effects of PFT-α on BBB integrity in MACO/R rats. Brain water content (**A**) and Evans blue permeability assay (**B**) for DKK1 and PFT-α effects on BBB in MCAO/R rats on day 7 of MCAO/R. Detection of mRNA levels of endothelial junction protein Zo-1 (**C**), Occludin (**D**), and Claudin-5 (**E**) in rat brain by RT-qPCR on day 7 of MCAO/R. $n = 4$; $^{***}P < 0.001$ vs. Sham; $^{\#\#\#}P < 0.001$ vs. MCAO/R; $^{\&\&}P < 0.01$, $^{\&\&\&}P < 0.001$ vs. MCAO/R + PFT-α

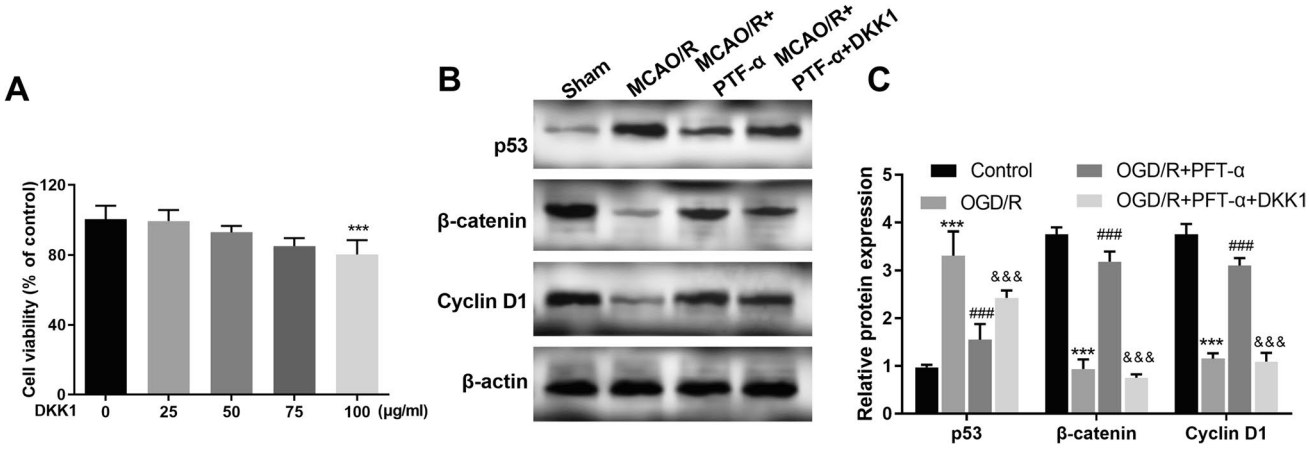

Fig. 4 DKK1 reversed the regulation of p53 and WNT signaling pathway key protein of PFT-α in OGD/R. **A** CCK-8 assays for cell viability in NSCs with OGD/R exposed to progressively increasing DKK1. **B**–**C** Western-Blot assay was performed to detect the protein levels of DKK1 on p53, β-catenin, and Cyclin D1 in NSCs with OGD/R. $n = 4$; $^{***}P < 0.001$ vs. control; $^{\#\#\#}P < 0.001$ vs. OGD/R; $^{\&\&}P < 0.01$, $^{\&\&\&}P < 0.001$ vs. OGD/R + PFT-α

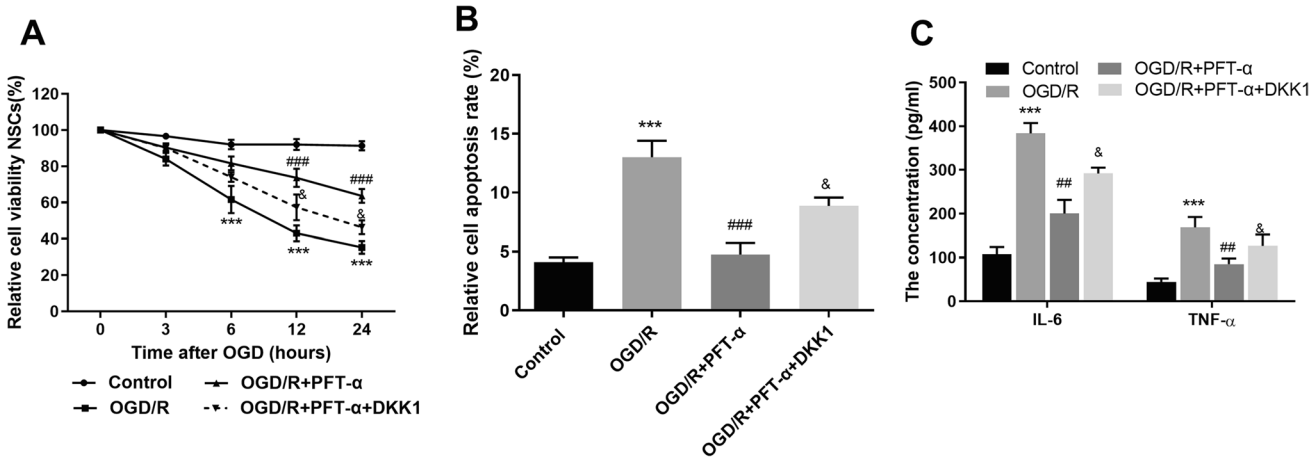

Fig. 5 DKK1 weakened the protection of PFT-α on the cellular function of NSCs with OGD/R. **A** CCK-8 assays were employed to examine cell viability in NSCs after OGD/R and PFT-α treatment with the addition of DKK1. Flow cytometry and ELISA to examine apoptosis (**B**), inflammation levels (**C**) in NSCs after OGD/R and PFT-α treatment with the addition of DKK1. $n = 5$; $^{***}P < 0.001$ vs. control; $^{\#\#}P < 0.01$, $^{\#\#\#}P < 0.001$ vs. OGD/R; $^{\&}P < 0.05$ vs. OGD/R + PFT-α

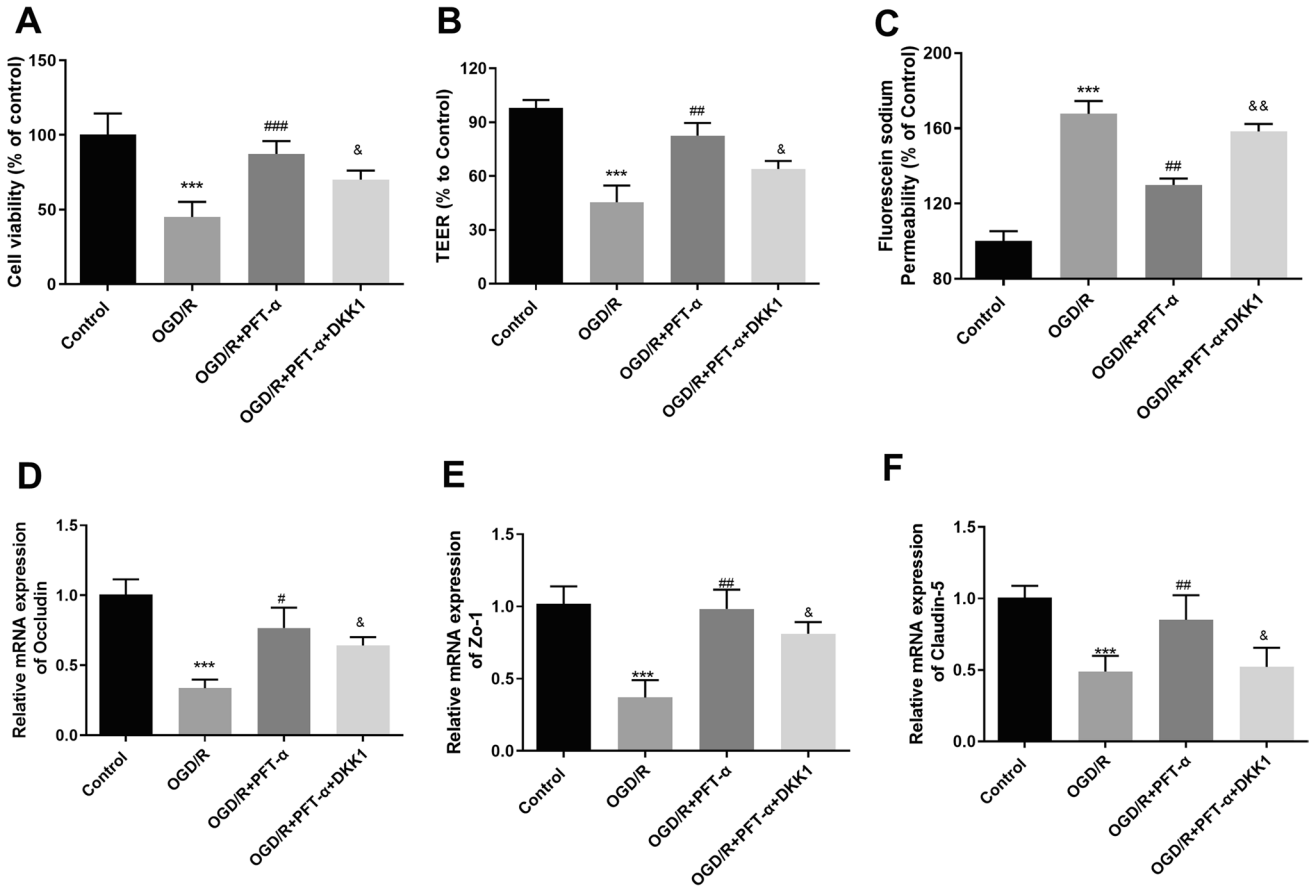

Fig. 6 DKK1 weakened the protection of PFT-α against the permeability of OGD/R-induced HBMECs. **A** CCK-8 was performed to resolve the viability of PFT-α as well as DKK1 on OGD/R-induced HBMECs. TEER value (**B**) and sodium fluorescein (**C**) were carried out to explore the permeability of HBMEC cells. mRNA levels of tight junctions occluded (**D**), Zo-1 (**E**), and claudin-5 (**F**) in DKK1 and PFT-α-induced OGD/R cells. $n = 5$; $^{***}P < 0.001$ vs. control; $^{\#}P < 0.05$, $^{\#\#}P < 0.01$, $^{\#\#\#}P < 0.001$ vs. OGD/R; $^{\&}P < 0.05$, $^{\&\&}P < 0.01$ vs. OGD/R + PFT-α

of function of p53 is frequently coupled with the activation of the classical WNT signaling pathway cascade (Kim et al. 2011). Therefore, in exploring the possible mechanism underlying the neuroprotective effect of suppressed p53 on CI/R injury, we focused our attention on the WNT signaling pathway and postulated that the activation of the canonical WNT signaling pathway might occur after p53 loss-of-function thereby ameliorating CI/R injury. The WNT signaling pathway exhibits functional abnormalities associated with malformed embryos, neurodegenerative diseases, cancer, and cardiovascular diseases (Ren et al. 2019). The ameliorative effect of WNT on CI/R injury was found. Morin is involved in mitigating neurological deficits and moto deficits in CI/R injury by mediating angiogenesis through modulation of the WNT signaling pathway (Khamchai et al. 2022). In the classical WNT signaling pathway, WNT binds to the receptor FZD to activate intracellular DSH protein and transmit it to the cell to inhibit the kinase activity of APC, GSK-3β, AXIN, and β-catenin forming complexes, thus causing the accumulation of β-catenin, and eventually initiating the transcription of target genes such as cyclin D1 and c-myc. Therefore, the key proteins cyclin D1 and β-catenin were selected for correlation in this study regarding the WNT signaling pathway. In the present research, we inhibited the activation of this signaling pathway by intracerebroventricular injection of DKK1, a WNT signaling pathway. Human recombinant protein DKK1, one of the four major secreted glycoproteins of the dickkopf family encoding 255-350 amino acids, was identified as the best-known WNT antagonist (Jiang et al. 2022). DKK1's C-terminus was identified as an essential and sufficient structural domain for WNT pathway inhibition, binds to LRP6, and antagonizes WNT signaling by triggering internalization of the receptor LRP5/6 (Jiang et al. 2022, Hong et al. 2018). In this study, we found that DKK1 inhibited the attenuating effect of PFT-α on p53 and restored the potential role of p53 in CI/R injury.

CI/R injury pathogenesis is extremely complex, involving the influence of multiple factors such as neurotoxicity, inflammatory response, and apoptosis (Shen et al. 2016).

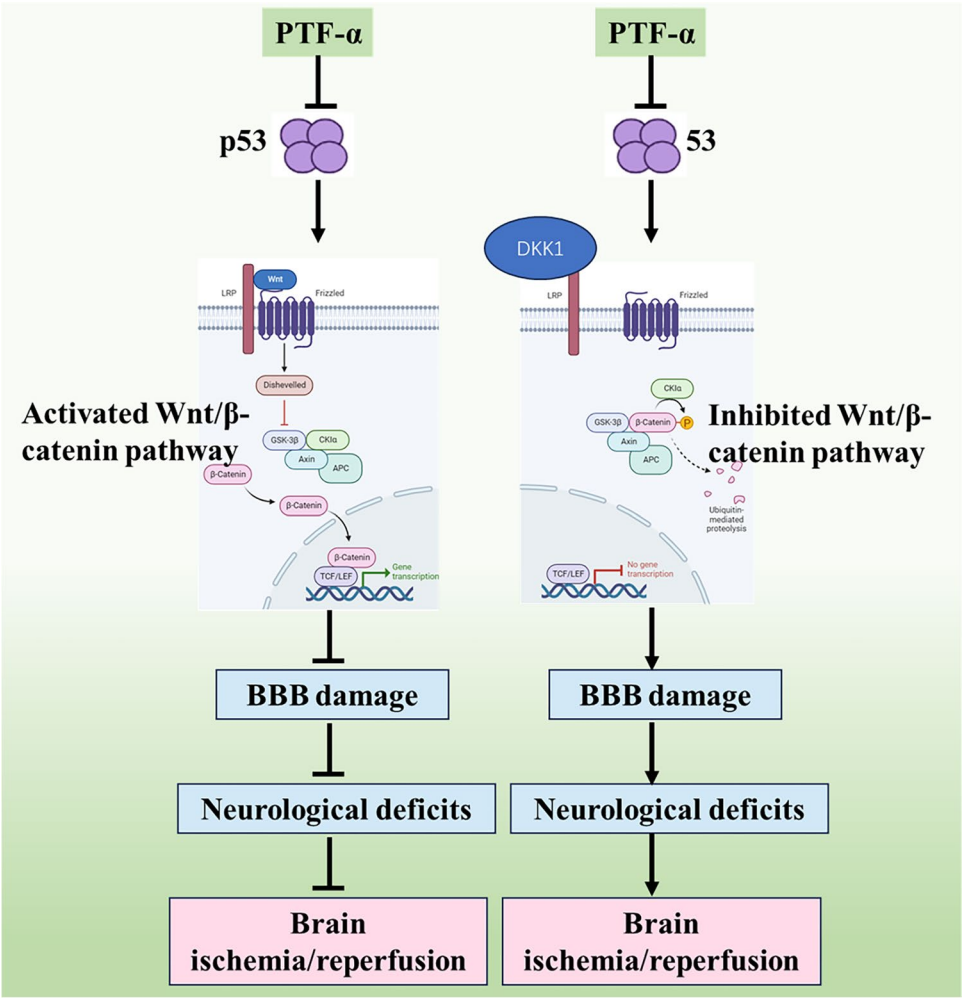

Fig. 7 PFT-α inhibits p53 to activate the Wnt/β-catenin pathway through the protection of the cerebral ischemic barrier, and then inhibits neurological deficits thereby alleviating cerebral ischemia-reperfusion injury, but this is significantly reversed by DKK1

In this study, we demonstrated that PFT-α significantly inhibited neurological deficits, brain infarct volume, neuronal apoptosis, and neuroinflammation in MCAO/R rats; exerted neuroprotective effects; and promoted the expression of β-catenin and Cyclin D1. However, DKK1 diminished the protective effect of PFT-α. In in vivo studies, we found that inhibition of p53 may exert a neuroprotective effect on CI/R injury by activating the WNT signaling pathway. In an in vitro study, the same results were obtained for NSCs isolated from fetal rats and subjected to OGD/R experiments simulating the onset of CI/R injury. Under OGD/R conditions, the cell viability of NSCs gradually decreased with increasing DKK1 concentration. Although this is inconsistent with Liu et al.'s finding in 2013 that DKK1 inhibited apoptosis in rat hippocampal neurons (Liu et al. 2013), we agree with Lrene's finding that DKK1 is necessary for the induction of ischemic neuronal death (Cappuccio et al. 2005), as well as Bortolasci et al.'s finding that DKK1 inhibits cell proliferation of NSCs (Bortolasci et al. 2020). Meanwhile, DKK1 attenuated the inhibitory effect of PFT-α on apoptosis in OGD/R cells. Overall, consistent with in vivo findings, DKK1 increased the levels of p53 expression and weakened the protective effect of PFT-α on CI/R injury.

The dysfunction of BBB plays a pivotal role in the occurrence of brain injury and subsequent neurological deficits following ischemic stroke. BBB is considered a predominant site of blood-central nervous system exchange at the level of the cerebral microvascular endothelium, and the main features of BBB injury after stroke are loss of tight junction integrity and altered expression of the associated protein, and increased paracellular permeability, leading to serious pathological consequences (Chen et al. 2018). Tight junctions are multimolecular complexes close to the apical membranes that are essential for the creation of paracellular barriers of highly resistant molecules and ions and the maintenance of barrier integrity, they consist of transmembrane proteins occludin, claudines-1, 3, 5, and are major determinants of tight junctional permeability, attached to the action cytoskeleton by scaffolding proteins Zo-1, Zo-2 and Zo-3 (Harati et al. 2022). In our study, we found that BBB permeability was increased in MCAO, while Zo-1, claudines-5, and occludin levels were decreased; that is, BBB integrity was disrupted, but PFT-α increased BBB permeability and enhanced the level of tight junction protein, exerting a protective effect on BBB integrity. In contrast, DKK1 eliminated the protective effect of PFT-α (Fig. 7). The same results were observed in HBMEC cells of OGD/R decreased endothelial resistance and increased paracellular permeability, whereas PFT-α typically reversed these effects, but this reversal was typically abrogated by DKK1. Finally, the present study comes with some limitations. The chloral hydrate and cervical subluxation we used to be not the optimal anesthesia. This problem improves in our next in-depth study.

In conclusion, our study confirms that suppressive p53 may protect the BBB after acute ischemic stroke by activating the WNT signaling pathway thereby exerting CI/R injury neuroprotective effects. This study may provide new insights and an experimental basis for CI/R injury management as well as clinically applied pharmacotherapy.

Supplementary Information The online version contains supplementary material available at https://doi.org/10.1007/s10142-023-01237-3.

Author contributions HTZ, DYD, and XNG conceptualized and designed the study. XLT, YQX, and BW collected, organized, and drafted the information. All authors analyzed the data. HTZ, DYD, and XNG wrote the manuscript. SJY, PFL, and ZFL performed manuscript revision. All the authors have read and approved the manuscript.

Funding This study was funded by the Natural Science Foundation of Shandong Province (No. ZR2020QH104) and Science and Technology Program of Binzhou Medical University (No. BY2018KJ06).

Data availability All data generated or analyzed during this study are included in this article. Further enquiries can be directed to the corresponding author.

Declarations

Ethics approval Animal care was conducted in compliance with the Guidelines for Care and Use of Laboratory Animals issued by the Ministry of Science and Technology of China, and the experimental protocols were passed by the Binzhou Medical University Hospital Animals Care and Use Committee. Every effort was made to reduce the number of animals as well as their suffering.

Informed consent n/a

Consent for publication n/a

Competing interests The authors declare no competing interests.

References

Beni FA, Kazemi M, Dianat-Moghadam H, Behjati M (2022) MicroRNAs regulating Wnt signaling pathway in colorectal cancer: biological implications and clinical potentials. Funct Integr Genomics 22:1073–1088. https://doi.org/10.1007/s10142-022-00908-x

Bortolasci CC, Spolding B, Kidnapillai S, Connor T, Truong TT, Liu ZS, Panizzutti B, Richardson MF, Gray L, Berk M, Dean OM (2020) Transcriptional effects of psychoactive drugs on genes involved in neurogenesis. Int J Mol Sci 21:8333. https://doi.org/10.3390/ijms21218333

Cao G, Jiang N, Hu Y, Zhang Y, Wang G, Yin M, Ma X, Zhou K, Qi J, Yu B, Kou J (2016) Ruscogenin attenuates cerebral ischemia-induced blood-brain barrier dysfunction by suppressing TXNIP/NLRP3 inflammasome activation and the MAPK pathway. Int J Mol Sci 17:1418. https://doi.org/10.3390/ijms17091418

Cappuccio I, Calderone A, Busceti CL, Biagioni F, Pontarelli F, Bruno V, Storto M, Terstappen GT, Gaviraghi G, Fornai F, Battaglia G (2005) Induction of Dickkopf-1, a negative modulator

of the Wnt pathway, is required for the development of ischemic neuronal death. J Neurosci 25:2647–2657. https://doi.org/10.1523/JNEUROSCI.5230-04.2005

Chang J, Mancuso MR, Maier C, Liang X, Yuki K, Yang LU, Kwong JW, Wang J, Rao V, Vallon M, Kosinski C et al (2017) Gpr124 is essential for blood-brain barrier integrity in central nervous system disease. Nat Med 23:450–460. https://doi.org/10.1038/nm.4309

Chen C, Huang Y, Xia P, Zhang F, Li L, Wang E, Guo Q, Ye Z (2021a) Long noncoding RNA Meg3 mediates ferroptosis induced by oxygen and glucose deprivation combined with hyperglycemia in rat brain microvascular endothelial cells, through modulating the p53/GPX4 axis. Eur J Histochem 65. https://doi.org/10.4081/ejh.2021.3224

Chen F, Liu Z, Peng W, Gao Z, Ouyang H, Yan T et al (2018) Activation of EphA4 induced by EphrinA1 exacerbates disruption of the blood-brain barrier following cerebral ischemia-reperfusion via the Rho/ROCK signaling pathway. Exp Ther Med 16:2651–2658. https://doi.org/10.3892/etm.2018.6460

Chen W, Jiang L, Hu Y, Fang G, Yang B, Li J et al (2021b) Nanomedicines, an emerging therapeutic regimen for treatment of ischemic cerebral stroke: a review. J Control Release 340:342–360. https://doi.org/10.1016/j.jconrel.2021.10.020

Guo H, Fan Z, Wang S, Ma L, Wang J, Yu D et al (2021) Astrocytic A1/A2 paradigm participates in glycogen mobilization mediated neuroprotection on reperfusion injury after ischemic stroke. J Neuroinflammation 18:230. https://doi.org/10.1186/s12974-021-02284-y

Harati R, Hammad S, Tlili A, Mahfood M, Mabondzo A, Hamoudi R (2022) miR-27a-3p regulates expression of intercellular junctions at the brain endothelium and controls the endothelial barrier permeability. PLoS One 17:e0262152. https://doi.org/10.1371/journal.pone.0262152

Hong SA, Yoo SH, Lee HH, Sun S, Won HS, Kim O et al (2018) Prognostic value of Dickkopf-1 and ss-catenin expression in advanced gastric cancer. BMC Cancer 18:506. https://doi.org/10.1186/s12885-018-4420-8

Hou JB, Shen QN, Wan X, Liu XK, Yu Y, Li M et al (2021) Ubiquitin-specific protease 29 exacerbates cerebral ischemia-reperfusion injury in mice. Oxid Med Cell Longev 2021:6955628. https://doi.org/10.1155/2021/6955628

Huang P, Wan H, Shao C, Li C, Zhang L, He Y (2021) Recent advances in Chinese herbal medicine for cerebral ischemic reperfusion injury. Front Pharmacol 12:688596. https://doi.org/10.3389/fphar.2021.688596

Jiang H, Zhang Z, Yu Y, Chu HY, Yu S, Yao S et al (2022) Drug discovery of DKK1 inhibitors. Front Pharmacol 13:847387. https://doi.org/10.3389/fphar.2022.847387

Khamchai S, Chumboatong W, Hata J, Tocharus C, Suksamrarn A, Tocharus J (2022) Morin attenuated cerebral ischemia/reperfusion injury through promoting angiogenesis mediated by angiopoietin-1-Tie-2 axis and Wnt/beta-catenin pathway. Neurotox Res 40:14–25. https://doi.org/10.1007/s12640-021-00470-7

Kim NH, Kim HS, Kim NG, Lee I, Choi HS, Li XY et al (2011) p53 and microRNA-34 are suppressors of canonical Wnt signaling. Sci Signal 4:ra71. https://doi.org/10.1126/scisignal.2001744

Li J, Li B, Bu Y, Zhang H, Guo J, Hu J et al (2022a) Sertad1 induces neurological injury after ischemic stroke via the CDK4/p-Rb pathway. Mol Cells 45:216–230. https://doi.org/10.14348/molcells.2021.0071

Li SS, Hua XY, Zheng MX, Wu JJ, Ma ZZ, Xing XX et al (2022b) Electroacupuncture treatment improves motor function and neurological outcomes after cerebral ischemia/reperfusion injury. Neural Regen Res 17:1545–1555. https://doi.org/10.4103/1673-5374.330617

Lin Q, Ma Y, Chen Z, Hu J, Chen C, Fan Y et al (2020) Sestrin-2 regulates podocyte mitochondrial dysfunction and apoptosis under high-glucose conditions via AMPK. Int J Mol Med 45:1361–1372. https://doi.org/10.3892/ijmm.2020.4508

Liu B, Tang J, Li S, Zhang Y, Li Y, Dong X (2013) Involvement of the Wnt signaling pathway and cell apoptosis in the rat hippocampus following cerebral ischemia/reperfusion injury. Neural Regen Res 8:70–75. https://doi.org/10.3969/j.issn.1673-5374.2013.01.009

Liu D, Wang H, Zhang Y, Zhang Z (2020a) Protective effects of chlorogenic acid on cerebral ischemia/reperfusion injury rats by regulating oxidative stress-related Nrf2 pathway. Drug Des Devel Ther 14:51–60. https://doi.org/10.2147/DDDT.S228751

Liu Y, Wu X, Du D, Liu J, Zhang W, Gao Y et al (2021) p53 inhibition provides a pivotal protective effect against cerebral ischemia-reperfusion injury via the Wnt signaling pathway. Cerebrovasc Dis 50:682–690. https://doi.org/10.1159/000516889

Liu Y, Zhang J, Zan J, Zhang F, Liu G, Wu A (2020b) Lidocaine improves cerebral ischemia-reperfusion injury in rats through cAMP/PKA signaling pathway. Exp Ther Med 20:495–499. https://doi.org/10.3892/etm.2020.8688

Nakada-Honda N, Cui D, Matsuda S, Ikeda E (2021) Intravenous injection of cyclophilin A realizes the transient and reversible opening of barrier of neural vasculature through basigin in endothelial cells. Sci Rep 11:19391. https://doi.org/10.1038/s41598-021-98163-w

Nazarinia D, Sharifi M, Dolatshahi M, Nasseri Maleki S, Madani Neishaboori A, Aboutaleb N (2021) FoxO1 and Wnt/beta-catenin signaling pathway: molecular targets of human amniotic mesenchymal stem cells-derived conditioned medium (hAMSC-CM) in protection against cerebral ischemia/reperfusion injury. J Chem Neuroanat 112:101918. https://doi.org/10.1016/j.jchemneu.2021.101918

Pan J, Li X, Guo F, Yang Z, Zhang L, Yang C (2019) Ginkgetin attenuates cerebral ischemia-reperfusion induced autophagy and cell death via modulation of the NF-kappaB/p53 signaling pathway. Biosci Rep 39:BSR20191452. https://doi.org/10.1042/BSR20191452

Pandian J, Panneerpandian P, Sekar BT, Selvarasu K, Ganesan K (2022) OCT4-mediated transcription confers oncogenic advantage for a subset of gastric tumors with poor clinical outcome. Funct Integr Genomics 22:1345–1360. https://doi.org/10.1007/s10142-022-00894-0

Pu S, Jia C, Li Z, Zang Y (2022) Protective mechanism of proprotein convertase subtilisin-like kexin type 9 inhibitor on rats with middle cerebral artery occlusion-induced cerebral ischemic infarction. Comput Intell Neurosci 2022:4964262. https://doi.org/10.1155/2022/4964262

Qiao W, Zang Z, Li D, Shao S, Li Q, Liu Z (2023) Liensinine ameliorates ischemia-reperfusion-induced brain injury by inhibiting autophagy via PI3K/AKT signaling. Funct Integr Genomics 23:140. https://doi.org/10.1007/s10142-023-01063-7

Ren L, Chen H, Song J, Chen X, Lin C, Zhang X et al (2019) MiR-454-3p-Mediated Wnt/beta-catenin signaling antagonists suppression promotes breast cancer metastasis. Theranostics 9:449–465. https://doi.org/10.7150/thno.29055

Shen MH, Zhang CB, Zhang JH, Li PF (2016) Electroacupuncture attenuates cerebral ischemia and reperfusion injury in middle cerebral artery occlusion of rat via modulation of apoptosis, inflammation, oxidative stress, and excitotoxicity. Evid Based Complement Alternat Med 2016:9438650. https://doi.org/10.1155/2016/9438650

Shi Y, Yi Z, Zhao P, Xu Y, Pan P (2021) MicroRNA-532-5p protects against cerebral ischemia-reperfusion injury by directly targeting CXCL1. Aging (Albany NY) 13:11528–11541. https://doi.org/10.18632/aging.202846

Wan H, Yang Y, Li Z, Cheng L, Ding Z, Wan H et al (2021) Compatibility of ingredients of Danshen (Radix Salviae Miltiorrhizae) and Honghua (Flos Carthami) and their protective effects on cerebral ischemia-reperfusion injury in rats. Exp Ther Med 22:849. https://doi.org/10.3892/etm.2021.10281

Wen L, Liu L, Li J, Tong L, Zhang K, Zhang Q et al (2019) NDRG4 protects against cerebral ischemia injury by inhibiting p53-mediated apoptosis. Brain Res Bull 146:104–111. https://doi.org/10.1016/j.brainresbull.2018.12.010

Wisniewska MB (2013) Physiological role of beta-catenin/TCF signaling in neurons of the adult brain. Neurochem Res 38:1144–1155. https://doi.org/10.1007/s11064-013-0980-9

Xie J, Kittur FS, Li PA, Hung CY (2022) Rethinking the necessity of low glucose intervention for cerebral ischemia/reperfusion injury. Neural Regen Res 17:1397–1403. https://doi.org/10.4103/1673-5374.330592

Yang M, Sun Y, Xiao C, Ji K, Zhang M, He N et al (2019) Integrated analysis of the altered lncRNAs and mRNAs expression in 293T cells after ionizing radiation exposure. Int J Mol Sci 20:2968. https://doi.org/10.3390/ijms20122968

Zhang P, Lei X, Sun Y, Zhang H, Chang L, Li C et al (2016) Regenerative repair of Pifithrin-alpha in cerebral ischemia via VEGF dependent manner. Sci Rep 6:26295. https://doi.org/10.1038/srep26295

Zhang QG, Wang R, Khan M, Mahesh V, Brann DW (2008) Role of Dickkopf-1, an antagonist of the Wnt/beta-catenin signaling pathway, in estrogen-induced neuroprotection and attenuation of tau phosphorylation. J Neurosci 28:8430–8441. https://doi.org/10.1523/JNEUROSCI.2752-08.2008

Publisher's Note Springer Nature remains neutral with regard to jurisdictional claims in published maps and institutional affiliations.

Springer Nature or its licensor (e.g. a society or other partner) holds exclusive rights to this article under a publishing agreement with the author(s) or other rightsholder(s); author self-archiving of the accepted manuscript version of this article is solely governed by the terms of such publishing agreement and applicable law.